Rapid structural remodeling of peripheral taste fibers is independent of taste cell turnover

Zachary D. Whiddon[1], Jaleia Marshall[1], David Alston[1], Aaron W. McGee[1], and Robin F. Krimm[1#]

[1]Department of Anatomical Sciences and Neurobiology, University of Louisville School of Medicine, Louisville, KY 40202

*These authors contributed equally to this work

[#]Correspondence to: Dr. Robin Krimm, MDR building, room 405B, 511 S. Floyd Street, Louisville, KY 40202

Key Words: taste, geniculate neuron, morphology, afferent, tongue

No. of Figures: 7
No. of Supplemental Figures: 1
No. of supplemental Tables: 0
No. of supplemental Movies: 1

ABSTRACT

Taste bud cells are constantly replaced in taste buds as old cells die and new cells migrate into the bud. The perception of taste relies on new taste bud cells integrating with existing neural circuitry, yet how these new cells connect with a taste ganglion neuron is unknown. Do taste ganglion neurons remodel to accommodate taste bud cell renewal? If so, how much of the taste axon structure is fixed and how much remodels? Here we measured the motility and branching of individual taste arbors (the portion of the axon innervating taste buds) over time with two-photon *in vivo* microscopy. Terminal branches of taste arbors continuously and rapidly remodel within the taste bud. This remodeling is faster than predicted by taste bud cell renewal, with terminal branches added and lost concurrently. Surprisingly, ablating new taste cells with chemotherapeutic agents revealed that remodeling of the terminal branches of taste arbors does not rely of the renewal of taste bud cells. Although the arbor structure remodeling was fast and intrinsically controlled, no new arbors were added, and few were lost over 100 days. Taste ganglion neurons maintain a stable number of nerve arbors that are each capable of high-speed remodeling. Arbor structural plasticity would permit arbors to locate new taste bud cells, while stability of arbor number could support constancy in the degree of connectivity and function for each neuron over time.

Introduction

The replacement of cells in the taste bud was discovered more than fifty years ago (Beidler and Smallman, 1965). In fact, cells within a taste bud are one of the fastest renewing cell populations in the body, with an average lifespan of 10 days (Beidler and Smallman, 1965; Farbman, 1980; Lindemann, 2001). Taste bud cells transduce chemical stimuli in the oral cavity, and transmit a signal to the axons of taste ganglion neurons, which carry this information to the brain. Each time a taste bud cell dies, the axon of a taste ganglion neuron must connect with a new taste bud cell if it is to maintain functional integrity (Hirose et al., 2020; Kumari et al., 2017; Lee et al., 2017). How this process is orchestrated is still unclear, but could involve structural remodeling of the neuron (Donnelly et al., 2022; Zaidi et al., 2016). Alternatively, taste bud cells could migrate to the axon of the taste ganglion neuron, making neuronal remodeling unnecessary.

Progress toward understanding the cellular movements occurring during taste bud cell turnover has been hindered by the use of fixed-tissue analysis (Beidler and Smallman, 1965; Farbman, 1980; Kinnamon et al., 1988; Wilson et al., 2022). Because cells are chemically fixed into position for observation, this approach fails to capture the dynamic processes within the taste bud, such as taste cell movements and axon remodeling. (Beidler and Smallman, 1965; Farbman, 1980; Ohman et al., in submission). Fixed-tissue studies also fail to describe what happens to axon remodeling when cell turnover is disrupted (e.g. chemotherapies) (Donnelly et al., 2022; Kumari et al., 2017, 2015). Additionally, because it is unknown whether taste ganglion neurons undergo structural remodeling, it is unclear why there are morphological differences between individual taste ganglion neurons (Huang et al., 2021). Morphological differences between

individual taste ganglion neurons could be inherent features of the neuron that dictate differences in functional properties or could be snap-shots in time of a continuously remodeling circuit that lacks functional stability. Understanding how taste ganglion neuron structure changes over time is a fundamental step in relating taste ganglion neuron morphology to function in the taste system.

In other parts of the nervous system, longitudinal *in vivo* imaging has been used to study the structural plasticity of axons and dendrites over time. Structural remodeling has been shown to occur during development and following injury or disease (Gangadharan et al., 2022; Martineau et al., 2018; Nakazawa et al., 2018; Speidel, 1935, 1933, 1932; Walsh and Lichtman, 2003). Under these conditions, axonal degeneration is the process that has been most extensively described (Bernstein and Lichtman, 1999; Bishop et al., 2004). In adult neurons, dendritic branches are mostly stable and remodeling is restricted to dendritic spine turnover (Grutzendler et al., 2002; Purves and Hadley, 1985; Trachtenberg et al., 2002). Axons may show a greater tendency to remodel than dendrites, but this remodeling is neuron type specific (De Paola et al., 2006). In the taste system, it has not been determined whether peripheral axons have the capacity remodel and to what extent remodeling occurs.

Here we examined the structure of peripheral taste axons using *in vivo* two-photon microscopy to determine how taste ganglion neuron structure changes over time. We discovered that peripheral axons of taste ganglion neurons have regions that rapidly remodel and regions that are stable throughout adulthood. Terminal branches remodel rapidly and axons undergo sufficient levels of remodeling to connect with new taste bud cells over time. The structural plasticity within taste ganglion neurons is an inherent

110 feature of the neurons and is not regulated by factors from the taste bud cells. Structural
111 stability maintains total number of axonal arbors for each taste ganglion neuron, and this
112 stability supports consistency in the total number of taste-transducing cells providing input
113 to an individual taste ganglion neuron. We conclude that taste ganglion neurons maintain
114 their peripheral circuits by having a stable number of axonal arbors, with each arbor
115 continuously remodeling to connect with new taste bud cells over time.

116 **Results**

117 **Acute *in vivo* imaging reveals axonal structural plasticity**

118 To determine whether axon structure in the peripheral taste system is fixed or
119 remodels over time, we developed an *in vivo* preparation to image the portion of the axon
120 of a taste ganglion neuron that terminates in the taste bud (axonal arbors). The arbors of
121 taste ganglion neurons enter taste buds in the epithelium. On the front two-thirds of the
122 mammalian tongue, taste buds are housed in epithelial structures called fungiform
123 papillae, which are easily accessible for imaging in live animals (Miller and Reedy, 1990).
124 Within taste buds, arbors form a dense plexus with many overlapping branches (Ohman-
125 Gault et al., 2017; Wilson et al., 2022). We used a sparse-labeling strategy to express
126 tdTomato in a small number of taste ganglion neurons so that individual arbors could be
127 distinguished (Huang et al., 2021). In this preparation, fewer than five labeled arbors were
128 labeled with tdTomato per fungiform taste bud and many taste buds did not contain any
129 labeled arbors. Individual arbors were imaged using two-photon laser scanning
130 microscopy (Figure 1A).

131 Individual arbors were imaged up to a depth of 70 microns to capture the entire
132 arbor, as well as a portion of the axon beneath the taste bud. To estimate the frequency
133 of structural plasticity for these axons, first we imaged the same arbors once per hour for
134 a 6 h period (n=36). We found that arbor structure within the lamina propria (Figure 1A,
135 purple dotted-line) of the fungiform papilla core was stable (Figure 1B, yellow box). Many
136 of the terminal branches of arbors within the taste bud (Figure 1A, green dotted line)
137 displayed structural changes in as quickly as a few hours after the initial imaging session
138 (Figure 1B, red box). Among the 36 arbors imaged, 24 changed their number of terminal
139 branches in a 6 h window by adding and/or subtracting small terminal branches (Figure
140 1B, yellow box).

141 To determine whether the very low excitation power (<51 mW) used for imaging
142 induced evident photobleaching, we imaged a new group of arbors (n=13 from two mice)
143 using identical acquisition parameters every hour for 6 h and compared the fluorescence
144 intensity across image stacks (z-max intensity projections) for the first and last timepoints.
145 We did not observe a significant decrease in average ($t(12) = -1.78$, $p = 0.076$) or
146 maximum ($t(12) = -1.78$, $p = 0.380$) fluorescence intensity despite imaging these
147 structures repeatedly (Figure 1C). Thus, this imaging approach was suitable for acute *in*
148 *vivo* imaging of individual axonal arbors and demonstrates that arbors of taste ganglion
149 neurons display high-speed structural remodeling.

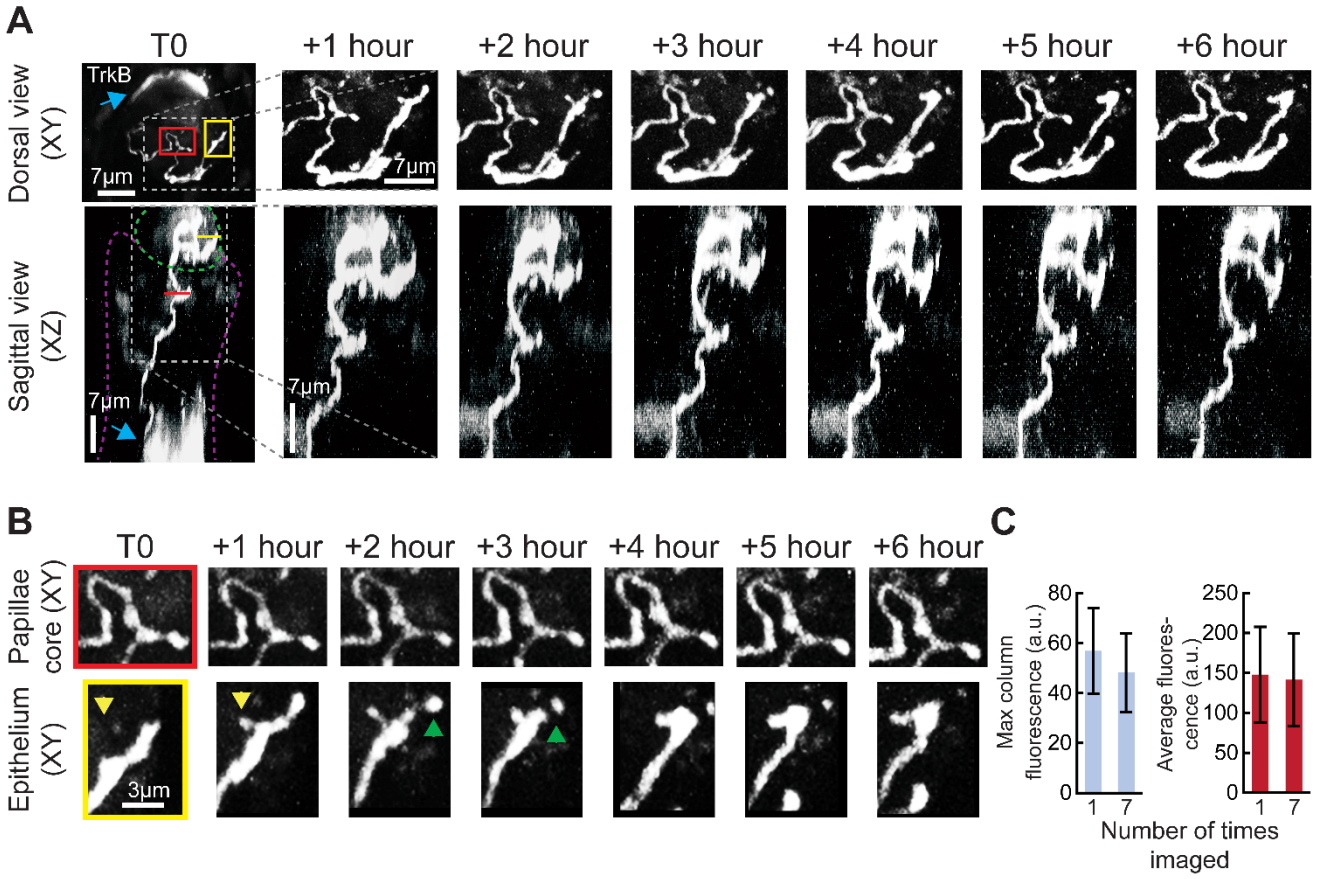

Figure 1. Intravital imaging of taste neurons in fungiform papillae. Example of a fungiform papilla with a single labeled receptive arbor illustrating the small-scale changes that can be seen within 6 hours. (**A**) Top and bottom rows show dorsal (XY) and sagittal (XZ) views of an arbor within a fungiform papilla every hour over a 6 h period. Some keratinocytes were also labeled (Liu et al., 2012; Tang et al., 2017) (cyan arrow). After T0, images for each consecutive timepoint are enlarged to show only the labeled arbor. At T0, the taste bud is outlined in a green dotted line, and the connective tissue core of the papilla is outlined in magenta. (**B**) High-magnification view (XY projection) of structural features of the arbor within the papilla core (red box) and taste bud (yellow box). The branch ending inside the taste bud bifurcated after 1 h and then reverted to a single branch ending after 4 h (yellow and green arrowheads). The portion of the arbor in the papilla core did not change across 6 h. (**C**) Average and maximum fluorescence (mean ±SD), using regions of interest around receptive arbors, in max intensity z-projections of arbors imaged every hour for 6 h. Fluorescence levels between hour 1 and 6 are unchanged.

Chronic *in vivo* imaging requires a fungiform papillae map

Next, we examined axonal structural plasticity over days. Reliably identifying the same taste buds across imaging sessions was critical for chronic imaging experiments.

154 To identify the same taste buds over days or weeks, we combined our approach for
155 sparse labeling of taste ganglion neurons (*Ntrk2*^{CreER} :tdTomato) with transgenic mice that
156 express green fluorescent protein (GFP) in taste buds (*Sox2*^{GFP}: Okubo et al., 2006).
157 When viewed at low-magnification, GFP expression on the anterior tongue surface
158 revealed a unique taste bud pattern for each mouse (Figure 2A) This provided a set of
159 fiduciary marks used to locate the same taste buds and arbors repeatedly over time.
160 Three taste buds in the example papillae map contained labeled arbors; they are shown
161 at high magnification 24 h apart (Figure 2B). No other fungiform taste buds viewed in this
162 field contained labeled arbors because of the sparseness of genetic labeling of taste
163 ganglion neurons (Figure 2A, taste buds with no box).

164 Taste bud cells have an average lifespan of 10 days (Beidler and Smallman, 1965).
165 Given this rate of taste bud cell turnover, we investigated the structural plasticity of arbors
166 every 12 h for 10 days. In five mice, we observed the same 31 taste buds and 60 labeled
167 arbors 21 times over 10 days. Among these arbors, four were lost during this period, and
168 none were added. One taste bud lost GFP expression in the epithelium, but the arbor
169 remained, consistent with taste bud loss due to aging (Liebl et al., 1999; Patel and Krimm,
170 2010). Examination of a single-labeled arbor at the beginning and end of the 10-day
171 experiment illustrates that arbor structure in the papillae core was stable, whereas arbor
172 structure in the epithelium was plastic (Figure 2C).

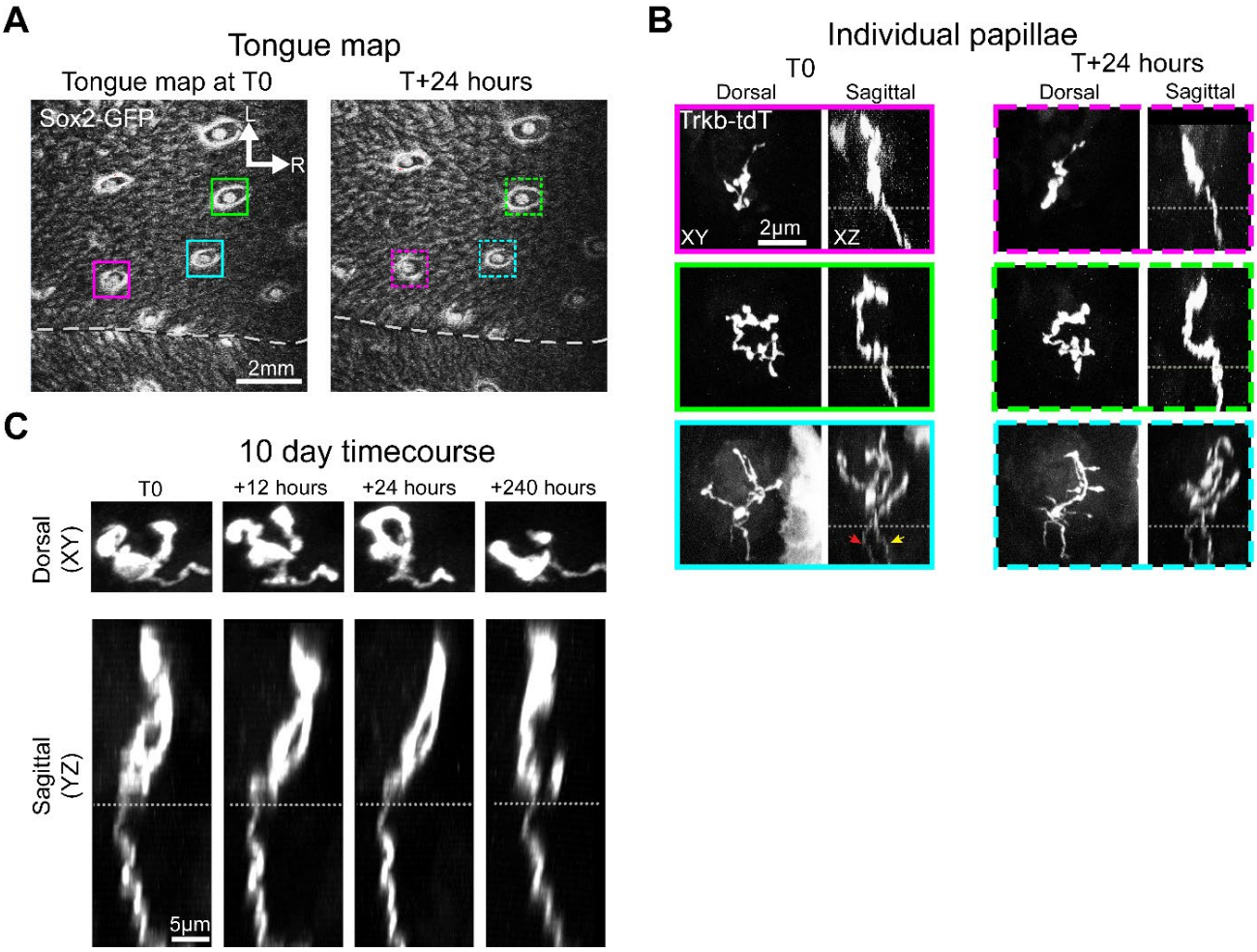

173

Figure 2. Chronic intravital imaging using a papillae map. (**A**) Sox2-GFP expression in the anterior tongue epithelium illustrating a papillae map. Papillae with labeled arbors are indicated by solid boxes at T0 and dashed boxes 24 h later. The tongue midline is indicated with a white dashed line, and rostral (R) and lateral (L) directions are indicated by white arrows. (**B**) High-magnification micrographs of TrkB-tdTomato-labeled nerve arbors in each of the three papillae indicated from the map. The first column shows the XY (dorsal) plane, which is parallel to the tongue surface, and the XZ plane is shown in the adjacent column. Gray dashed lines in the z-plane images illustrate the bottom of the taste bud. The papillae outlined in magenta and green have a single labeled arbor, and the papilla outlined in cyan has two separate labeled arbors (yellow and red arrows). Micrographs outlined in dashed lines show high-magnification views of the same papillae 24 h later. Some changes to each arbor structure can be seen during this time within the taste bud but not within the papillae core. (**C**) Receptive arbors were imaged every 12 h for 10 days, and an example arbor is shown at the initial timepoint (T0) as well as 12, 24, and 240 h later.

174 **Terminal branches remodel rapidly and continuously over 10 days**

175 The axonal arbors of taste ganglion neurons synapse with taste bud cells
176 (Kinnamon et al., 1988; Romanov et al., 2018; Vandenbeuch et al., 2015; Wilson et al.,
177 2022). Many taste axonal arbors contact taste bud cells on terminal branches (Ohman et
178 al., in submission). If the turnover of taste bud cells regulates arbor structure, then
179 terminal branches are likely to remodel as taste bud cells die and/or new cells enter the
180 taste bud. Arbors form synapses with an average of 1.6 taste bud cells (Kinnamon et al.,
181 1988). If new terminal branches are added and lost as a means of synapsing with new
182 taste bud cells, then most arbors should add or lose roughly one terminal branch over 10
183 days, and some arbors are likely to remain stable.

184 In five mice, we imaged 31 taste buds containing a total of 60 arbors. However,
185 taste buds with three or more labeled arbors were not quantified because we could not
186 distinguish arbors when branches intermingled. We identified 26 individual arbors from
187 21 different taste buds that were distinguishable at all timepoints and quantified their
188 terminal branches every 12 h (Figure 3A-B, video 1). All quantified arbors added and lost
189 multiple terminal branches during within 10 days (Figure 3B-C). In 43% of arbors, a
190 terminal branch was lost or added within the first 12 h, and 100% of arbors gained or lost
191 a branch within the first 4.5 days (108 h, Figure 3D). For the 30 arbors imaged every 12
192 h for at least 4 days, one terminal branch was added or lost every 16.8 ± 1.1 h. This
193 anatomical plasticity was much faster than predicted based on the rate of taste bud cell
194 turnover. Thus, terminal branches do not appear to be added for the primary purpose of
195 synapsing with a new taste bud cell or lost solely as a mechanism for disconnecting from
196 dying taste bud cells.

197 Given the high rate of terminal branch addition and removal, we suspected that we
198 could be underestimating the rate of change if some terminal branches were both gained
199 and lost within the 12 h intervals between imaging sessions. To test this possibility, we
200 imaged every 4 h for a 12 h period. For this image set (n = 57 arbors), an average of one
201 terminal branch was added or lost every 6.6 ± 1.0 h, which was a significantly faster rate
202 of change than the one obtained when arbors were imaged every 12 h (16.8 h; Figure
203 3E, U = 470.5, $p < 0.001$, Mann-Whitney U). These results indicate that imaging every 12
204 h underestimates the rate of terminal branch change. To verify the accuracy of this rate
205 of terminal branch change, we compared arbors imaged every 4 h to arbors imaged every
206 hour for 6 h (n = 36) and found no significant difference in the rate of terminal branch
207 gain/loss (1 h rate: 5.5 ± 0.8 h; 4 h rate, 6.6 ± 1.0 h; U = 822.5, $p = 0.09$) (Figure 3E).
208 Thus, we conclude that accurately describing changes in terminal branch number
209 requires sampling arbor structure every 4 h. However, given the high rate of terminal
210 branch addition and loss, we also sought to determine whether two-photon exposure
211 influences the rate of terminal branch addition/loss. We compared arbors imaged twice in
212 6 h with arbors imaged seven times over the same amount of time (Figure 3F). There was
213 no difference in the rate of change in terminal branch number over the 6 h period between
214 these two sets of arbors, indicating that image collection does not influence the rate at
215 which terminal branches are added and lost.

216

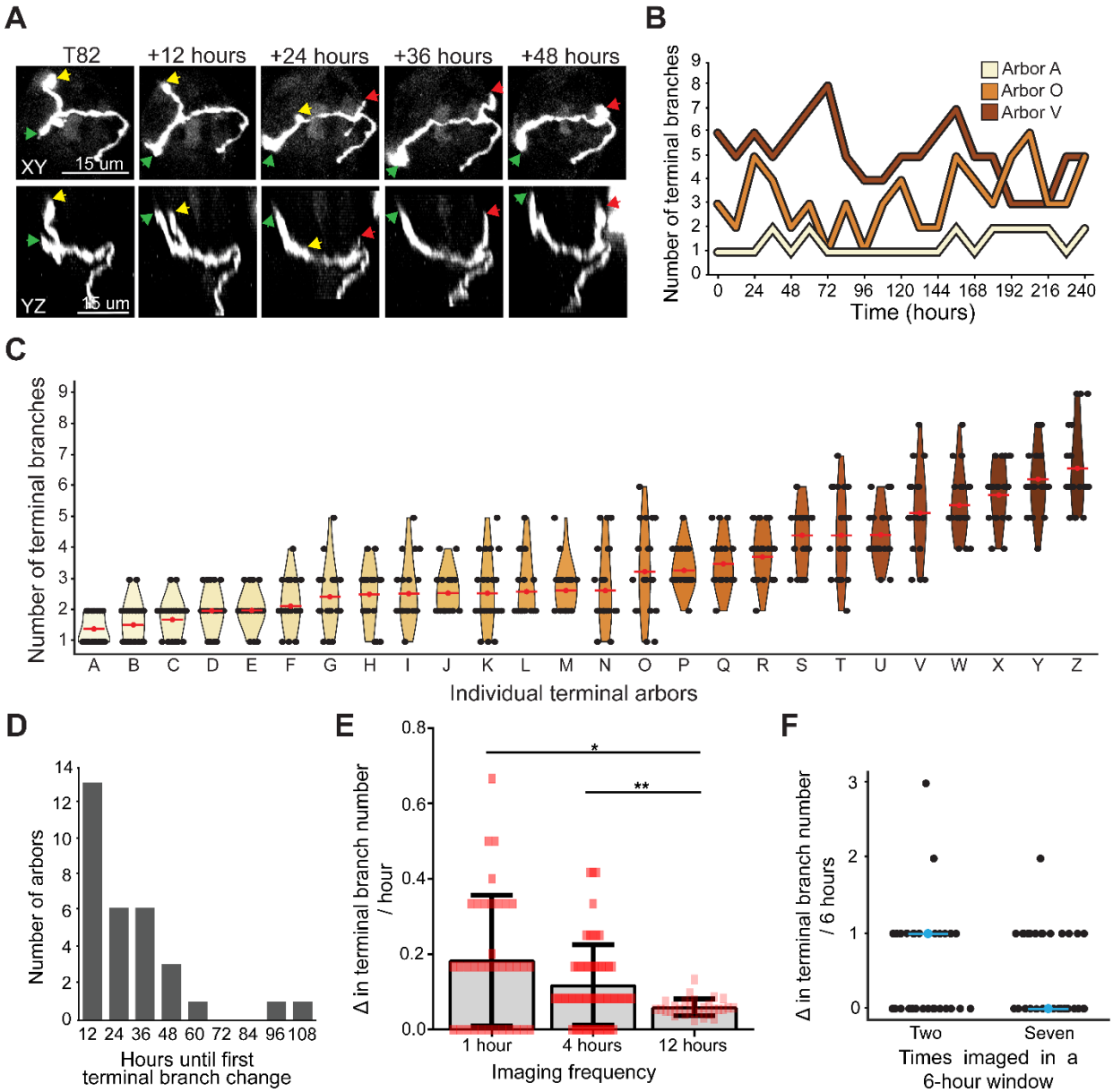

Figure 3. Terminal branches are continuously and rapidly remodeled. (**A**) Example arbor shown every 12 h over 2 days (for the full 10 days see Figure 3, see supplementary movie 1 for full 10 days). Terminal branches labeled with green and red arrowheads extended during this period, while the terminal branch labeled with a yellow arrowhead retracted. (**B**) Number of terminal branches every 12 h for three arbors across the 10-day imaging window. (**C**) Violin plots for 26 (A-Z) individual arbors showing the distribution of terminal branch number during the 10-day imaging window. Arbors are arranged in ascending order of average terminal branch number (red dot and bar) across 10 days. (**D**) Amount of time until the first gain or loss of a terminal branch. All arbors added or lost a terminal branch within 108 h. (**E**) Violin plots showing rates of change in terminal branch number per hour for three different sampling frequencies: 1, 4, or 12 h. Median values are indicated with cyan dots and bars (Single asterisk $p<0.05$, double $p<0.001$). (**F**) Rate of change in terminal branches over 6 h for arbors imaged twice compared with arbors imaged seven times. Median values are indicated with cyan dots and bars.

217

Gain/loss of terminal branches is not regulated by taste bud cell turnover

If arbors add new branches in order to synapse with new taste bud cells, then altering the rate of new cell entry would be expected to alter terminal branch dynamics. To test the hypothesis that taste ganglion neuron remodeling is dependent on the addition of new taste bud cells we prevented new cells from being added to taste buds by blocking Hh-signaling. Administering LDE225 (trade name Sonidegib) (Figure 4A) stops new taste cells from differentiating and entering taste buds (Castillo et al., 2014; Castillo-Azofeifa et al., 2017; Ermilov et al., 2016; Kumari et al., 2017, 2015; Lu et al., 2018) (Figure S1). This is a chemotherapeutic agent used to treat basal cell carcinoma and is associated with

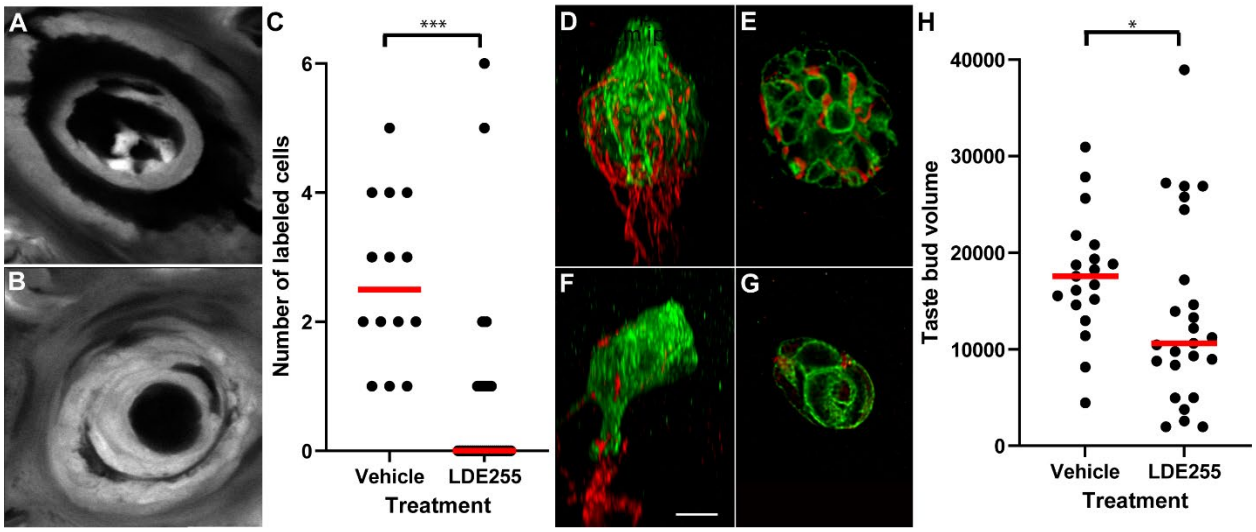

Figure 4 - Supplemental 1. LDE225 inhibits new cell entry into the taste bud, resulting in volume reduction by day 10. **A-C)** A subset of epidermal precursor and/or stem cells expressing K14-CreER:tdTomato were labeled with a single dose of tamoxifen immediately preceding 10 days of treatment with vehicle (**A**) or LDE225 (**B**). On day 10, LDE255-treated mice had fewer labeled cells in taste buds than vehicle-treated mice (**C**). Specifically, 27 of 40 taste buds completely lacked new labeled cells following LDE255 treatment, while all those examined had some labeled cells following vehicle treatment. (**D-H**) Whole mounts of the lingual epithelium were labeled for taste buds (green) and neurons (Phox2b-tdTomato, red) following 10-day of treatment with vehicle (**D** z-plane, **E** x-y plane) and LDE225 (**F** z-plane, **G** x-y plane) tongues. (**H**) Taste bud volumes were smaller following 10 days of LDE225 compared with vehicle controls. *$p \leq 0.05$, ***$p \leq 0.001$.

227 loss of taste by patients receiving treatment (Jacobsen et al., 2016; Kumari et al., 2015;
228 Lacouture et al., 2016; Tang et al., 2012).

229 We treated mice with LDE225 (n=4) or vehicle (n=2) for 10 days and imaged taste
230 axonal arbors every 4 h for 12 h on days 6, 8, and 10. Over time, old taste cells continue
231 to die and taste bud volume decreases (Castillo-Azofeifa et al., 2017) (Figure S1).
232 However, arbors had similar rates of terminal branch change on each day of imaging
233 ($H(30) = 29.5$, $p = 0.44$). Terminal branch gain/loss was similar between the LDE225 and
234 vehicle groups ($U = 312$, $p = 0.61$) (Figure 4B). Thus, we conclude that preventing new
235 cells from entering taste buds does not alter the rate of terminal branch remodeling.

236 We also examined how taste buds recover following treatment with LDE255. Many
237 fungiform papillae recovered normal taste bud morphology, however some failed to
238 recover and lacked Sox2 expression up to 40 days after treatment for 10 days with
239 LDE225 (Figure 4C). Non-recovered papillae retained taste ganglion neuron innervation
240 even in the absence of taste buds (Figure 4D). Surprisingly, we observed at least some
241 remodeling of terminal branches in all papillae that lacked taste buds over 20-day,
242 although remodeling over 24-hour was limited. Two example papillae with single labeled
243 arbors are shown in Figure 4E. We conclude from these findings that the taste bud is not
244 required for terminal branch remodeling of taste arbors, although remodeling may be
245 slowed.

246

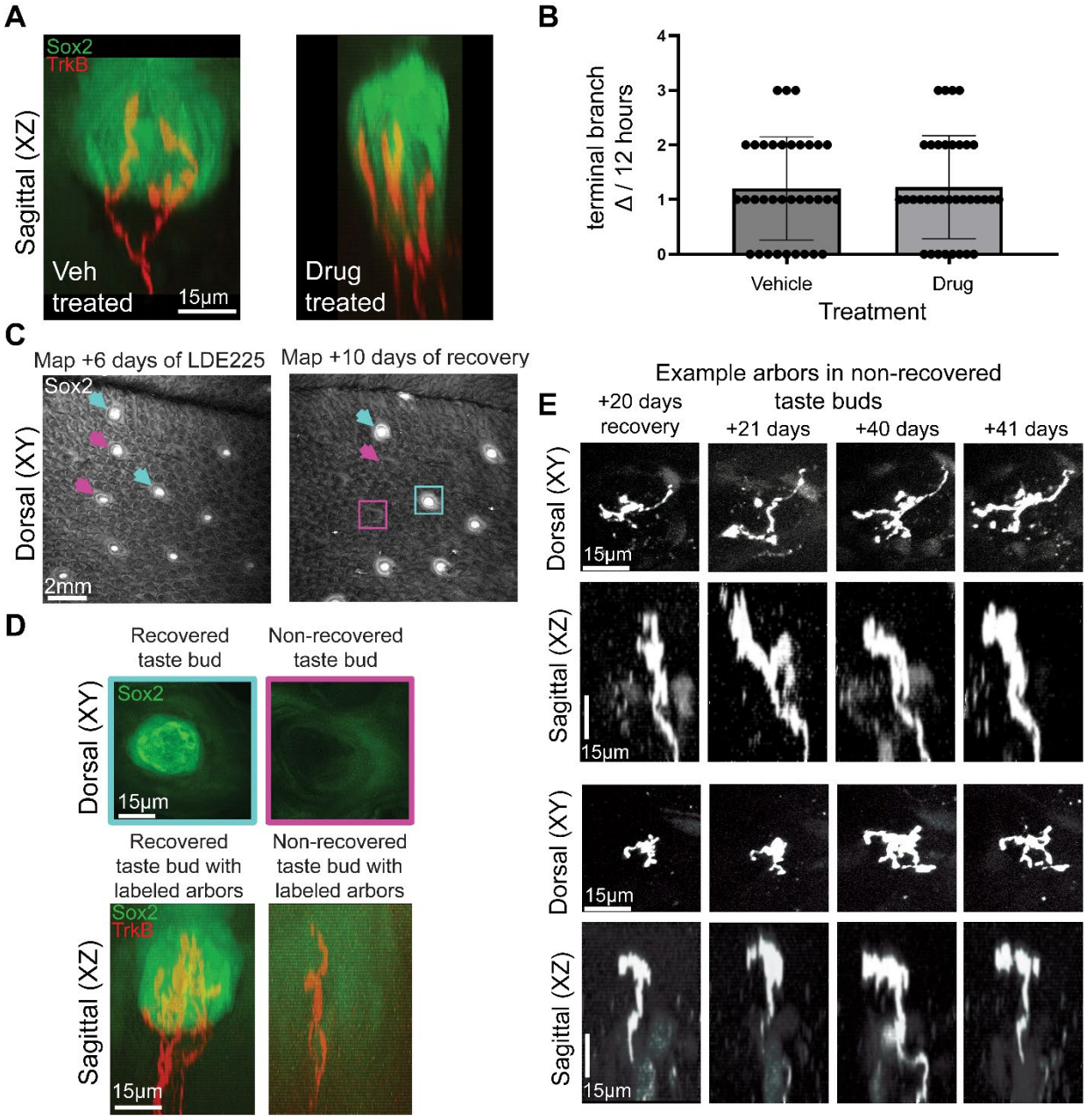

Figure 4. Terminal branch remodeling is not influenced by addition of new cells into the taste bud. (**A**) Example vehicle-treated and drug-treated taste buds after 8 days of treatment. (**B**) There was no difference in the rate with which terminal branches were gained/lost when taste bud cell turnover was halted (LDE225-treated mice) compared with normal conditions (vehicle-treated/untreated mice). (**C**) After LDE225 treatment, some fungiform papillae did not regain taste buds as determined by Sox2-GFP (magenta arrows and box). Two recovered taste buds are indicated with blue arrows and box. (**D**) Individual fungiform papillae with a taste bud had high levels of Sox2 expression, whereas papillae without a taste bud lacked cells with high levels of Sox2 expression. Papillae with both recovered and non-recovered taste buds retained taste ganglion neuron innervation. (**E**) Two papillae containing non-recovered taste buds with single-labeled arbors are shown 20, 21, 40, and 41 days after LDE225 treatment. Both arbors continued to remodel somewhat despite the absence of a taste bud.

247

248 **Growth and retraction occur concurrently within the arbor**

249 Some terminal branches displayed distinct morphologies as swellings on the tip of
250 the terminal branch, as well as punctate swellings along the axon (Figure 5A). We
251 suspected these features could be associated with remodeling, as both retraction bulbs
252 and growth cones have been described in taste arbors (Zaidi et al., 2016). To determine
253 if terminal branch swellings were associated with gain or loss of terminal branches, we
254 examined 12 arbors from three mice that were imaged every 12 h for 10 days (n = 252
255 total timepoints). We observed 72 instances of swellings at the tip of the terminal branch
256 and/or branch swellings long the branch. These terminal swellings along the axon were
257 followed by retraction of the branch 86.1% of the time, whereas only 13.9% of terminal
258 branches displayed terminal branch swelling without retracting (Figure 5B). Therefore, we
259 conclude that terminal end swellings are often associated with retracting terminal
260 branches (Figure 5A).

261 Since not all branch loss is associated with a retraction bulb, one possibility is that
262 only those retractions with a retraction bulb occur when taste cells are lost. To determine
263 if this was the case, we examined the frequency of retractions which were associated with
264 retraction bulbs. Retractions with retraction bulbs occurred at a frequency of once per 40
265 h and was also faster than the rate predicted by cell turnover. This finding indicates that
266 branches retract for reasons other than loss of taste bud cells.

267 We next investigated whether retractions associated with retraction bulbs
268 contributed to reduced arbor size by comparing the volume occupied by the arbor (convex
269 hull; Figure 5C) and arbor length (Figure 5D) before and after terminal branch retraction.
270 Retraction of a single terminal branch did not alter total arbor size (Student's unpaired t-

271 test, t=0.4515, df=74, p=0.65). These lost branches may represent a small percentage of
272 the total branch length. Consistently, the average length of retraction for a single branch
273 identified using end bulbs and beading was 14.1± 11.9 μm (Figure 5E), which was a small
274 portion of the total length of these arbors (mean=79.2 ± 40.8 μm). In addition, branch
275 elongation also commonly occurred in the arbor at another location concurrently with
276 terminal branch retraction. Consistently, 21 of 38 arbors increased in total length while
277 retracting a terminal branch. These opposing changes in branch length maintain arbor
278 size over time.

279 Given that arbors add and lose terminal branches concurrently to maintain size,
280 we wondered to what extent the total range of arbor complexity, measured as terminal
281 branch number, changed in each arbor over 10 days. We observed that most arbors
282 maintained a limited range of complexity over 10 days (Figure 5F), such that the minimum
283 and maximum number of terminal branches for each arbor was correlated (Figure 5G, R^2
284 = 0.698, $p < 0.001$). Simple arbors (1-3 branches) did not become complex (more than 6
285 branches) within a 10-day window. Although large branch retractions also occurred
286 frequently within 10 days, they occurred simultaneously with terminal branch formation,
287 which limited the range of complexity for most arbors.

288

289

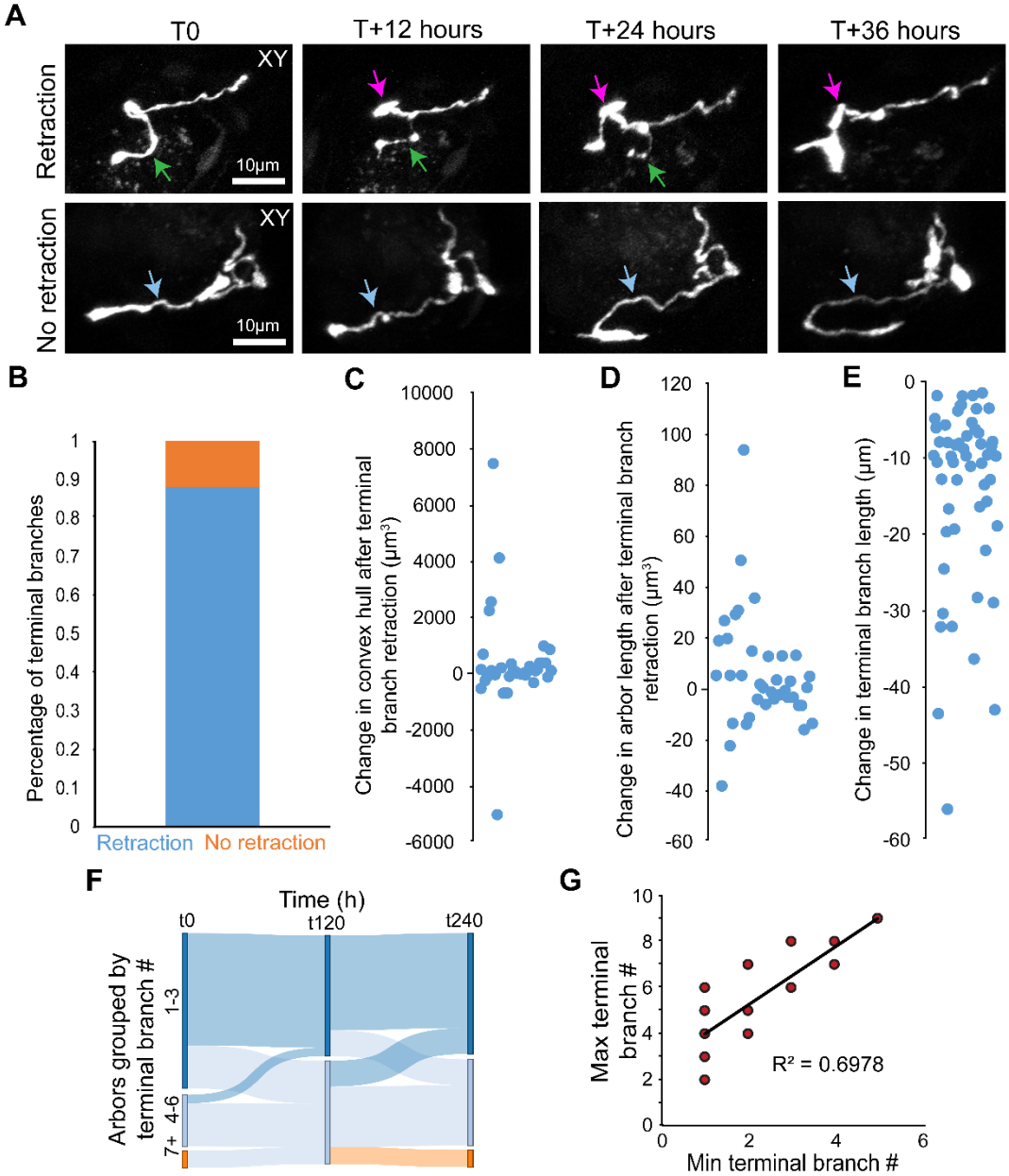

Figure 5. Morphologic changes predict terminal branch retraction but not change in arbor size. (**A**) Two example arbors shown across a 36 h window. In the top row, a terminal branch retracted after displaying a bulb at the tip of the ending and swellings within the branch (green arrow). A separate terminal branch on this same arbor extended (magenta arrow) in conjunction with terminal branch retraction. In the bottom row, a terminal branch displayed an end-bulb and swellings but did not retract (blue arrow); instead, it extended, indicating that the bulb may have been a growth cone. (**B**) Most terminal branches that displayed end-bulbs and swellings retracted at later timepoints (blue); however, a small portion did not retract (orange). (**C**) Change in convex hull after each terminal branch retraction. (**D**) Net change in total arbor length after each terminal branch retraction. (**E**) Change in terminal branch length. (**F**) Sankey diagram showing arbors grouped based on total number of terminal branches (1 to 3 = dark blue, 4 to 6 = light blue, 7+ = orange). Most arbors did not change groups at 5 (t120) or 10 (t240) days of imaging, demonstrating some stability in arbor complexity over time. (**G**) Correlation between minimum and maximum number of terminal branches for 26 receptive arbors observed every 12 h for 10 days.

291 **Variability in arbor size over 10 days differs across arbors**

292 Because arbor size (convex hull) was not heavily impacted by the retraction of
293 single terminal branches we hypothesized that arbor size is maintained despite constant
294 arbor remodeling. To determine if this was the case, we examined whether arbor size
295 (convex hull and total arbor length) changed over 10 days. To perform comparisons
296 across all timepoints within a 10-day period, we developed a semi-automated image
297 analysis pipeline in MATLAB, called ArborTools, to segment arbors and quantify convex
298 hull and total arbor length (Figure 6A). Reconstructions of each arbor were verified
299 visually to confirm that the arbor and the reconstruction matched (Figure 6, cyan vs white).
300 Arbors with too much background noise for automatic tracing were removed from
301 analysis. The volume occupied by the arbor (convex hull) changed in the taste bud across
302 10 days. In general, convex hull changed along with total length (Figure 6C). These
303 changes in size could be due to changes in height, or x or y width, or combinations of
304 these changes (Figure 6D). For example, the illustrated arbor (Figure 6 A-C), increases
305 in size occur due to an increase in Y-width from 0 to 12 hours, but dramatically increases
306 in size between hour 228-240 due to concurrent increases X, Y width and height.

307 When examining the extent to which individual arbors displayed changes in size,
308 we noticed that some arbors appear to be more variable (Figure 6D). We divided them
309 into two groups based on the variability of their sizes over 10 days (Figure 6E, insert).
310 Arbors appear to divide into those that vary little over time and remain small, and those
311 that remodel more extensively (Figure 6E). Those that remodel more extensively are also
312 larger on average over 10 days. These two groups could represent phases in a

remodeling cycle that extends beyond 10 days, or it could represent two distinct populations of taste arbors that differ is regard to degree of remodeling.

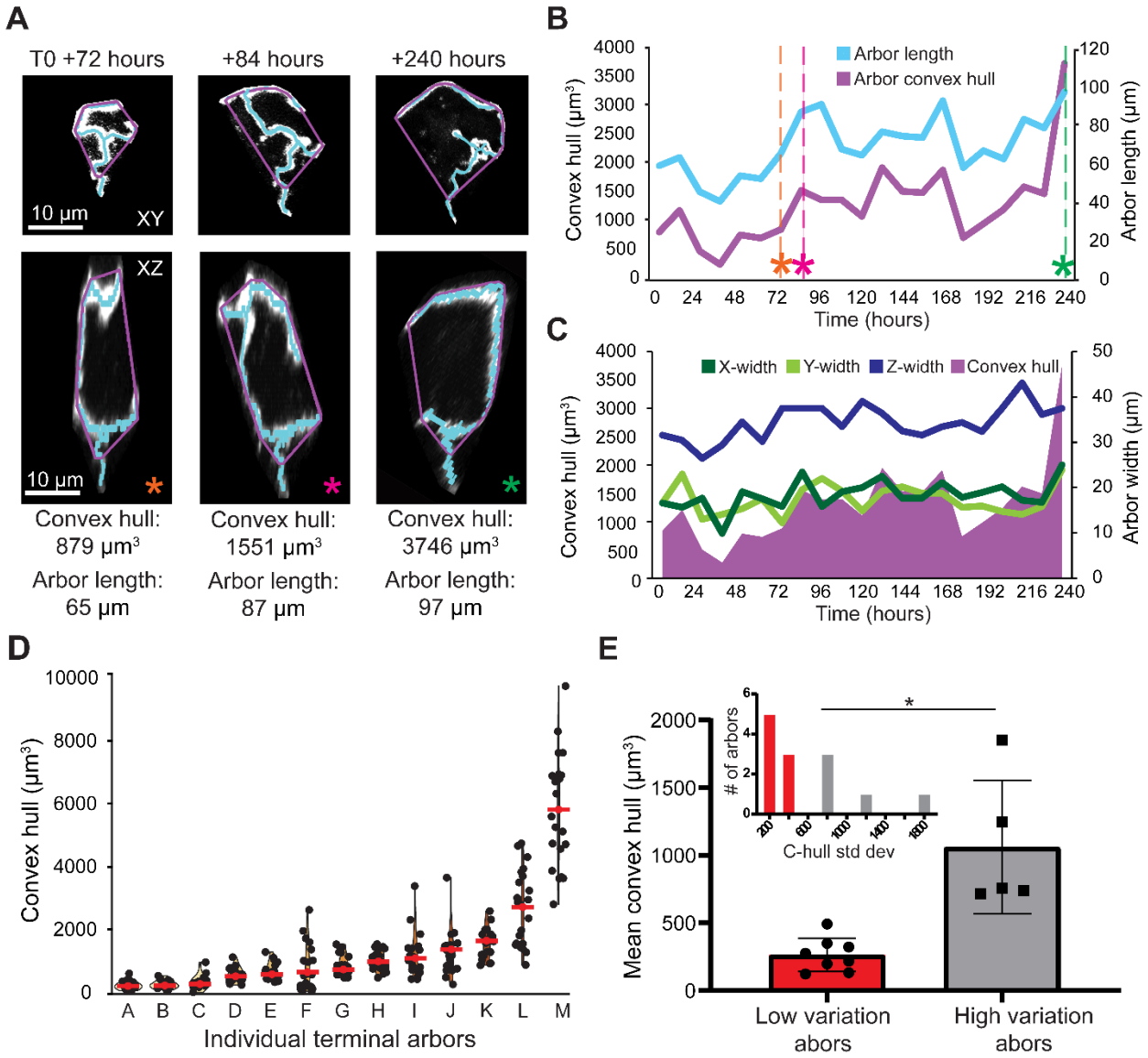

Figure 6. Taste neuron arbors vary in size over 10 days. A custom image analysis pipeline was developed to segment arbor structure from raw image TIF stacks. (**A**) Examples of convex hulls (purple) and arbor skeletons (cyan) generated from segmentation data are shown in two orientations and at three timepoints. Colored asterisks at each timepoint are used to indicate convex hull and arbor length in (C). (**B**) Convex hull size (purple line) and arbor length (cyan) for the example arbor in (A) are shown across the entire 10-day imaging window. **(C)** Convex hull potted with Z-height, x-width and y-width over time. (**D**) Convex hull measured for 13 individual arbors arranged by ascending average size. Average convex hull and arbor length during the 10-day imaging window are indicated with red dots and bars. **(E)** Within 10 days small arbors remodel little and are small, while other remodel more extensively and tend to be larger and more variant in size.

315 **Number of arbors within a taste bud is stable over 100 days**

316 Within 10-days, we did not observe any new arbors growing into taste buds, and
317 only a small number of arbors were lost. Therefore, total number of arbors may be a stable
318 feature for a given taste ganglion neuron over time. Alternatively, gain loss of whole arbors
319 may occur, but require a longer time than 10 days. To distinguish between these
320 possibilities, we imaged taste buds every 10 days for 60 or 100 days in mice where
321 neurons were sparsely labeled. We observed taste buds with labeled arbors (n = 18 for
322 60 days, n = 13 for 100 days) as well as buds without labeled arbors (n = 18 for 60 days,
323 n = 13 for 100 days) (Figure 7A). The arbor structure in the papillae core was largely
324 unchanged over 100 days (Figure 7B, purple dotted line). In addition, no taste buds
325 acquired new labeled arbors in 60 or 100 days of imaging. Initially, 18 taste buds
326 contained a total of 33 labeled arbors. After 60 days of imaging, 31 arbors were still
327 present. No additional labeled arbors were lost from the remaining taste buds throughout
328 the 100 days (Figure 7C). These results suggest that the number of arbors is a stable
329 feature of the neuron in adulthood. Arbors do not exhibit the full range of complexity over
330 100 days (Figure 7D). Convex hull and arbor length also indicate that some arbors remain
331 small, while others are more variable (Figure 7E-F).

332

333

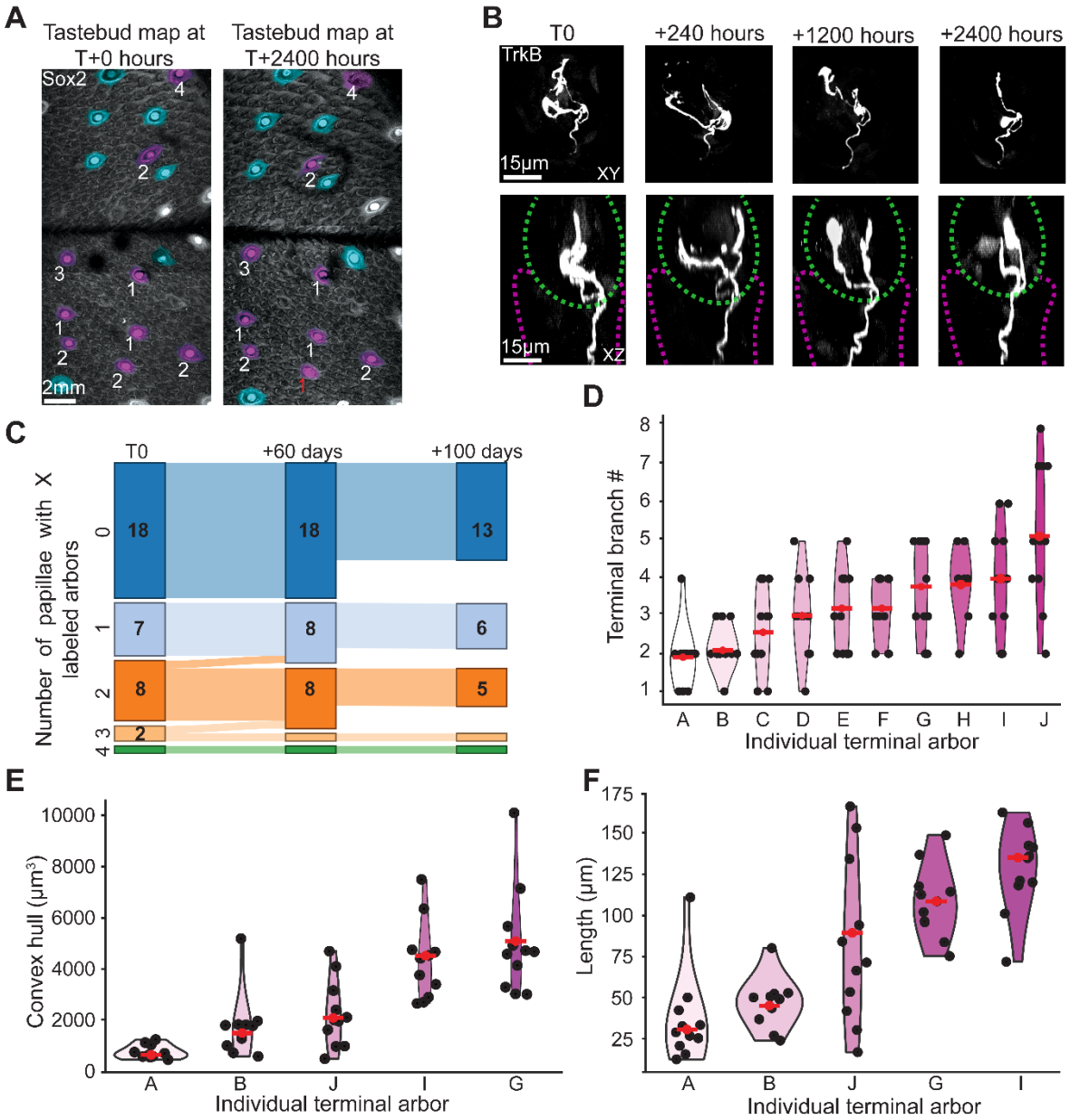

Figure 7. Arbor number is stable over 100 days. (**A**) Two papillae maps of the same regions shown 100 days apart. Purple taste buds contained labeled arbors (number of arbors labeled in white), and blue taste buds did not contain labeled arbors. One papilla in this map lost an arbor during the 100-day window (red label). (**B**) Example arbor at days 0, 10, 50, and 100. The taste bud is outlined in a green dotted line and papillae core in magenta. (**C**) Taste buds were categorized by number of labeled arbors and plotted in a Sankey diagram. No taste buds acquired new arbors, and two taste buds lost an arbor during the first 60 days. One mouse was not imaged past day 60. (**D**) Violin plots of terminal branch number for 10 arbors imaged every 10 days for 100 days. Average number of terminal branches during the 100-day window are indicated with red dots and bars. Violin plots of convex hull (**E**) and arbor length (**F**) for five individual arbors imaged every 10 days for 100 days. Arbor identities are conserved from (**D**).

335 **Discussion**

336 Taste bud cells are continuously replaced through adulthood (Beidler and
337 Smallman, 1965; Farbman, 1980; Hamamichi et al., 2006), but whether taste ganglion
338 neurons remodel while reconnecting with new taste bud cells was unknown. In other
339 systems, intra-vital imaging has been used to examine neuron remodeling during
340 development, following injury, and in some cases during adulthood (Breton-Provencher
341 et al., 2016; De Paola et al., 2006; Marshall et al., 2016; Nakazawa et al., 2018; Pfeiffer
342 et al., 2018; Speidel, 1933, 1932; Takahashi et al., 2019; Trachtenberg et al., 2002; Verzé
343 et al., 1999; Walsh and Lichtman, 2003). Here we show that all peripheral taste axons
344 have arbors that continuously remodel, and compared to plasticity in other systems, do
345 so with unprecedented speed. For example, a structure well-studied for its remodeling
346 capabilities in adulthood, the dendritic spine, remodels over days (Pfeiffer et al., 2018),
347 and at least half of the observed spines are stable over months (Grutzendler et al., 2002;
348 Trachtenberg et al., 2002). In contrast to dendritic spines, some terminal branches of taste
349 axonal arbors appear and leave over much shorter time-scales – sometimes lasting less
350 than 12 hours. The speed and extent of remodeling in peripheral taste axons provides
351 insight into two basic questions. First, how do nerve arbors locate a new taste bud cell
352 during the process taste cell renewal? Secondly, is morphological variation across
353 individual peripheral axons due entirely to plasticity, or can taste neurons be classified as
354 distinct types based on anatomical differences? We discuss each of these issues.

355 **The relationship between taste arbor remodeling and cell renewal.**

356 Most taste arbors only connect to one taste bud cell at any given time (Kinnamon
357 et al., 1988; Wilson et al., 2022). In a 10-day period roughly half of the population of taste

358 bud cells turnover. Therefore, we anticipated that approximately half of all arbors sampled
359 would lose their connection to a bud cell and/or gain a new connection within 10-days.
360 We expected that arbor structure would be stable while connected to a taste bud cell,
361 remodeling only when connections were broken (Ohman et al., submitted). This type of
362 phasic remodeling is observed in terminal arbors of touch neurons that receive input from
363 Merkel cells (Marshall et al., 2016). The results of our study do not support the model that
364 taste neurons experience distinct phases of remodeling and stability; rather the arbors of
365 taste ganglion neurons continuously remodel with concurrent terminal branch growth and
366 retraction, similar to the pattern of remodeling in touch terminals of ear-skin (Takahashi
367 et al., 2019).

368 During remodeling, the arbors of taste ganglion neurons display similar anatomical
369 features to motor axon terminals, which innervate neuromuscular junctions, and undergo
370 remodeling as refinement occurs during development. However, refinement largely
371 consists of terminal branch retraction and pruning (Bishop et al., 2004; Walsh and
372 Lichtman, 2003). Motor axon retraction is typically accompanied by retraction bulbs and
373 terminal branch swellings. In addition to refinement, these features are also seen during
374 degeneration after injury (Bernstein and Lichtman, 1999; Bishop et al., 2004; Erturk et al.,
375 2007). Similarly, the axonal arbors of taste ganglion neurons have also been described
376 as having these irregular swellings and end-bulbs (Zaidi et al., 2016). Here, we found that
377 branches displaying these features are indeed in the process of retracting. These
378 observations suggest that retraction occurs by a conserved mechanism across systems
379 – a process that involves axosomal vesicle shedding and engulfment of neuronal debris
380 by phagocytic cells (Bishop et al., 2004). In the case of motor neurons, there is evidence

381 that factors provided from the neuromuscular junction trigger terminal branch retraction
382 (Bernstein and Lichtman, 1999). While the anticipated source of such a signal in the taste
383 bud would be from a dying taste bud cell, retraction occurs more frequently than would
384 be predicted based on the rate at which cells are leaving the taste bud. The frequency of
385 terminal branch retractions suggests that a signal from a dying taste bud cell is not
386 required to trigger terminal branch retraction in taste neuron terminal arbors.

387 Taste bud cells release growth and guidance factors, and as new cells enter the
388 taste bud they could release factors that stimulate branch formation and/or extension
389 (Donnelly et al., 2018; Lee et al., 2017; Meng et al., 2015; Nosrat et al., 2012; Sukumaran
390 et al., 2017; Treffy et al., 2016; Yee et al., 2003). However, our finding that terminal branch
391 remodeling is much faster than expected based on the rate of cell turnover is not
392 consistent with this possibility. Instead, terminal branch remodeling may be an intrinsic
393 feature of taste ganglion neurons, occurring regardless of what external factors are
394 present. To assess whether this remodeling is driven by an intrinsic mechanism, we
395 examined remodeling of terminal arbors while preventing addition of new cells into taste
396 buds. Treatment with LDE225 inhibits taste bud cell differentiation such that new taste
397 bud cells do not enter the taste bud (Castillo-Azofeifa et al., 2017; Kumari et al., 2015).
398 Surprisingly, we found that preventing integration of new taste bud cells does not
399 influence the frequency of terminal branch loss or formation. In fact, we observed that
400 taste arbors remain and continue to remodel even after the entire taste bud was lost. This
401 finding is consistent with the presence of growth associated protein-43 (GAP43) in the
402 arbors following treatment with LDE225 (Donnelly et al., 2022). Collectively, these

403 findings support the conclusion that axonal arbor remodeling is an intrinsic characteristic
404 of peripheral taste neurons.

405 Previously, we hypothesized taste arbors remodel to connect with new taste cells
406 over time (Ohman and Krimm, 2021). This model assumed that taste bud cells provide
407 an extrinsic signal to influence arbor remodeling. Because this concept is not supported
408 experimentally by the current study, we offer an updated model of how taste nerve fibers
409 connect to new taste bud cells over time. We propose that axonal arbors of taste ganglion
410 neurons continuously sample the taste bud compartment by extending and retracting
411 terminal branches, and this remodeling is orchestrated by an intrinsic cellular mechanism.
412 An intrinsic program that drives constant remodeling allows taste arbors to detect
413 extracellular signals and compare spatial arrangements of taste cells in their immediate
414 environment. By extending branches randomly and continuously nerve arbors eventually
415 come near to a cell of the "correct type". Once it is in the vicinity of the new taste bud cell,
416 trophic mechanisms may attract the taste arbor a short distance to the cell. Furthermore,
417 if constant terminal branch remodeling causes a terminal arbor to come in contact with a
418 cell, then detection of surface molecules, such as protocadherin could regulate the
419 connection, and growth factors may be unnecessary (Hirose et al., 2020). In this scenario,
420 terminal branch remodeling orchestrates the detection of extrinsic molecular cues and is
421 not a response by peripheral taste neurons to extrinsic molecular cues.

422 **The role of plasticity in individual peripheral taste axon morphology.**

423 A primary goal of the current study was to determine which structural features of
424 peripheral taste neurons are plastic and which features are stable. Addressing this
425 question is fundamental in determining whether taste neurons can be classified

426 morphologically into separate types (Dvoryanchikov et al., 2017; Zhang et al., 2019).
427 Taste neurons are pseudo-unipolar sensory neurons with a single axon and a primary
428 bifurcation that creates a central and peripheral projection (Yarmolinsky et al., 2009; Zaidi
429 and Whitehead, 2006). We recently described the morphology of taste neurons for the
430 first time using a fixed-tissue approach (Huang et al., 2021). The peripheral axons of taste
431 neurons vary considerably in structure due to differences in the number of branch points
432 within the tongue muscle, the lamina propria and within the taste bud (Huang et al., 2021).
433 Here we show that the taste arbors remodel, and the number terminal branches for an
434 individual axonal arbor is determined by plasticity.

435 Although terminal branches remodel quickly, the gain and loss of terminal
436 branches occur concurrently, such that loss of a terminal branch does not always reflect
437 a decrease in arbor size. Individual arbor size does vary over time; however, some
438 individual arbors change in size more than others. We recently found that individual taste
439 neurons either have all small arbors, or have a mix of large and small arbors (Ohman et
440 al., in submission). It may be that degree of plasticity in an arbor size varies across
441 different types of taste neurons. Large arbors with higher degrees of plasticity likely probe
442 more of the taste bud environment, and are more likely to locate a scarce taste bud cell
443 type. So these type of endings could be specialized to neuron types that are narrowly-
444 tuned and require input from uncommon taste cell types.

445 Interestingly, the number of arbors labeled remained stable over 100 days. The
446 presence or absence of arbors in the bud is dictated by branch points within the axon that
447 are in the muscle or lamina propria. These branch points are not added and/or lost during
448 adulthood. Even when taste buds are eliminated, individual arbors remain in the location

449 previously occupied by taste buds. The axons of taste ganglion neurons may have
450 between 1 to 14 arbors (Huang et al., 2021). Given that most arbors only connect to 1-2
451 cells, the number of arbors is the primary anatomical feature that determines how many
452 taste bud cells provide input to a given neuron (Wilson et al., 2022). Neurons with more
453 arbors are predicted to be both more sensitive and broadly tuned than neurons with fewer
454 arbors (Ohman and Krimm, 2021). Although there is evidence that peripheral taste
455 neurons can change function over time (Bradley et al., 1997), there is also likely some
456 level of functional stability so that taste information is relayed to the brain as an
457 interpretable code. Maintaining a constant number of arbors is one mechanism by which
458 taste neurons could maintain functional stability over time.

459 Here, we determined that some anatomical features of peripheral taste axons are
460 highly plastic while others display long-term stability. Stable anatomical features of taste
461 ganglion neurons that also vary across neurons could define morphological neuron types.
462 These stable morphological differences may correspond to genetically defined neuron
463 types (Dvoryanchikov et al., 2017; Zhang et al., 2019) or functional differences (Barretto
464 et al., 2015; Lundy and Contreras, 1999; Wu et al., 2015). However, It is still unclear
465 whether peripheral taste neuron types are defined by a combination of expression,
466 function, and stable morphological features (Zeng and Sanes, 2017). By describing which
467 portions of taste axons are plastic and which are stable, we are now poised to determine
468 if stable morphological features differ across genetic or functional types.

469

470 **Materials and methods**

471 **Animals**

472 All animals were cared for in accordance with guidelines set by the United States
473 Public Health Service Policy on the Humane Care and Use of Laboratory Animals and
474 the National Institutes of Health Guide for the Care and Use of Laboratory Animals.

475 *TrkB*^{CreER} mice (*Ntrk2*$^{tm3.1(cre/ERT2)Ddg}$; ; ISMR catalog #JAX:027214,
476 RRID:IMSR_JAX:027214) were crossed with Cre-dependent tdTomato mice (Rutlin et al.,
477 2014; RRID: IMSR_JAX:007914) to obtain *TrkB*^{CreER}:tdTomato mice in which tdTomato
478 is expressed following TrkB-driven Cre-mediated gene recombination. These mice were
479 crossed with a Sox2-GFP line (Sox2^{tm2Hoch};; ISMR catalog #JAX:017592,
480 RRID:IMSR_JAX:017592). Phox2b-Cre mice (MRRC_034613-UCD) were also bred with
481 tdTomato reporter mice for fixed tissue experiments. K14^{CreERT} mice; ISMR catalog
482 #JAX:005107, RRID:IMSR_JAX:005107) were crossed with tdTomato reporter mice for
483 lineage tracing of taste cells. For all experiments, mice were postnatal day 60 or older at
484 the initial imaging session. Males and females were used across all *in vivo* experiments
485 (24 males and 19 females in total). Mice were divided across experiments as follows: 10-
486 day imaging (n = 5), 100-day imaging (n = 3). 4 h imaging (n = 5) 1 h imaging (n = 4), 6-
487 h imaging (n = 2), 4 h live imaging Hh-inhibition (n = 6; vehicle n = 2, LDE225 n = 4), new
488 cells entering the taste bud (n = 7; vehicle n = 2, LDE225 n = 5), confocal imaging
489 experiments examining taste bud size (n = 10; vehicle n = 5, LDE225 n = 5).

490 **Tamoxifen administration**

491 Tamoxifen (T5648, MiliporeSigma, St. Louis, MO) was dissolved in corn oil (C-
492 8267, MiliporeSigma) at 20 mg/ml by shaking and heating at 42°C and injected in a single
493 dose on postnatal day 40 by intragastric gavage.

494 **LDE225 administration**

495 Mice were treated by daily oral gavage for 10, 16, or 23 days with vehicle (PEG
496 400:5% dextrose in water) or LDE225 (NVP-LDE225, ChemieTek, Indianapolis, IN)
497 dissolved in vehicle at a dose of 20 mg/kg. The dose was determined based on Kumari
498 et al. (2015) and preliminary studies. The oral gavage probe (22-gauge, 25 mm; Instech)
499 by-passed all oral tissues for direct delivery into the stomach.

500 **Immunohistochemistry**

501 Phox2b-Cre:tdTomato mice were killed by avertin overdose (4 mg/kg) and
502 perfused transcardially with 4% paraformaldehyde. Dissected tissues were postfixed in
503 4% paraformaldehyde for 2 h (for thin serial sections) or overnight (thick sections and
504 whole mounts), rinsed with PBS, and transferred to 30% sucrose at 4°C overnight. A razor
505 blade was used to remove the anterior two-thirds of the tongue, after which tongues were
506 carefully split down the midline with a razor blade under a dissection microscope.
507 Tongues were frozen the next day in OCT and stored at -80°C before processing for
508 whole-mount staining. Whole-mount immunohistochemistry of the lingual epithelium was
509 performed to visualize innervated taste buds. First, the underlying muscle and lamina
510 propria were removed as described previously (Ohman and Krimm, 2021). The isolated
511 lingual epithelium was then washed for 15 min (three times) in 0.1 M PBS. Tissues were
512 then incubated in blocking solution (3% donkey serum and 0.5% Triton X-100 in

513 0.1 M PBS) at 4°C overnight and then incubated for 5 days at 4°C with primary antibodies
514 (DsRed (rabbit) and Troma1 (rat)) in antibody solution (0.5% Triton X-100 in 0.1 M PBS).
515 Tissues were rinsed four times for 15 min each with 0.1 M PBS and incubated with
516 secondary antibodies anti-DsRed (1:500; RRID:AB_10013483; Living Colors DsRed
517 polyclonal; Takara Bio USA, San Jose, CA) and anti-Troma1 (1:500, Alexa Fluor 488
518 AffiniPure, RRID:AB_2340619; Jackson ImmunoResearch, West Grove, PA). Tissues
519 were then rinsed again, mounted with Fluoromount-G, and coverslipped (high precision,
520 0107242; Marienfeld).

521 **Confocal imaging**

522 Taste bud images were obtained using an Olympus Fluoview FV1000 confocal
523 laser-scanning microscope with a 60× NA1.4 lens objective using a zoom of 3, Kalman 2.
524 Image sizes were initially set at 1024 × 1024 pixels but were cropped to reduce scanning
525 time and bleaching. Serial optical sections at intervals of 0.47 μm in the Z dimension were
526 captured, which is the optimal size at 60× magnification for 3D reconstruction. All colors
527 were imaged sequentially in separate channels to avoid bleed-through. Image stacks
528 were then deconvolved using AutoQuant X3 software (Media Cybernetics, Rockville, MD)
529 to reduce out-of-focus fluorescence and improve image quality.

530 **Two-photon *in vivo* imaging**

531 *In vivo* 2PLSM imaging was performed using a movable objective microscope
532 (Sutter Instruments, Novato, CA). A Fidelity-2 1070-nm laser (Coherent, Silicon Valley
533 was used to visualize tdTomato, and a Chameleon tunable laser (Coherent) set to 920
534 nm was used to visualize GFP. A custom-built tongue holder, based on a published

535 design, was used to stabilize the anterior tongue for imaging of the dorsal surface (Han
536 and Choi, 2018). Mice were anesthetized using a 0.6% isoflurane (Henry Schien, Melville,
537 NY) and O_2 mixture. A temperature controller was used to monitor and maintain body
538 temperature at 36°C. Ophthalmic lubricant ointment (Henry Schien) was applied to the
539 eyes. Taste bud maps were acquired using a 10 × 0.3 numerical aperture water
540 immersion objective lens (Carl Zeiss, USA), and images of receptive arbors were
541 acquired using a 40 × 10 numerical aperture water immersion lens (Zeiss). An early
542 version of ScanImage (Matlab) was used to collect images. Receptive arbors were
543 typically imaged to 70 microns in depth below the surface of the tongue, and 80 × 80 μm
544 optical sections (512 × 512 pixels) were collected at 0.5 or 1 μm increments.

545 **Image analysis**

546 Taste bud volume was calculated by contouring whole-mount-stained taste buds
547 at 3 micron increments perpendicular to the XY plane of the confocal z-stack. K14 cells
548 were manually quantified from taste bud z-stacks using ImageJ. Terminal branches of
549 sparsely labeled receptive arbors were manually quantified from z-stacks using ImageJ.
550 Terminal branches that displayed retraction bulbs were quantified using the SNT plugin.
551 A custom Matlab program (ArborTools, Github link to software will go here) was used to
552 automatically segment arbors. 3D images stacks were cropped to isolate terminal arbors
553 from background. A custom filter was used to extract initial segmentation volumes (Lang
554 et al., 2011). After automatic segmentation, the segmented arbors were compared to the
555 arbors and instances where background pixels were segmented were manually selected
556 to not be included in the convex hull and length analysis. From segmented volumes

557 skeletons were extracted using the Treestoolbox (Cuntz et al., 2010). All convex hull and
558 arbor length data reported were generated from ArborTools.

559 **Statistical analysis**

560 Rates of terminal branch change were compared across image sets by first testing
561 whether the measure was normally distributed using a Shapiro-Wilk test. If a measure
562 was normally distributed, then differences were determined using a Student's t-test for
563 two groups or one-way analysis of variance with a Tukey *post hoc* test for more than two
564 groups. If a measure was not normally distributed, then differences were determined
565 using a Mann-Whitney test for two groups or Kruskal-Wallis test for more than two groups.
566 A p-value <0.05 was used to determine statistical significance.

567 **Supplementary material**

568 S1 Movie. The arbor from Figure 3A (x-Y view) from T0-T228, every 12 hours = 0.5
569 seconds Time in hours is on the bottom right-hand side of the images. Branches are
570 added and lost to the portion of the arbor inside the taste bud.

571

572 **References**
573

574 AU - Ohman LC, AU - Krimm RF. 2021. Whole-Mount Staining, Visualization, and Analysis of Fungiform,
575 Circumvallate, and Palate Taste Buds. *J Vis Exp* e62126. doi:10.3791/62126
576 Barretto RPJ, Gillis-Smith S, Chandrashekar J, Yarmolinsky DA, Schnitzer MJ, Ryba NJP, Zuker CS. 2015.
577 The neural representation of taste quality at the periphery. *Nature* **517**:373–376.
578 doi:10.1038/nature13873
579 Beidler LM, Smallman RL. 1965. RENEWAL OF CELLS WITHIN TASTE BUDS. *J Cell Biol* **27**:263–272.
580 doi:10.1083/jcb.27.2.263
581 Bernstein M, Lichtman JW. 1999. Axonal atrophy: The retraction reaction. *Curr Opin Neurobiol* **9**:364–
582 370. doi:10.1016/S0959-4388(99)80053-1
583 Bishop DL, Misgeld T, Walsh MK, Gan W-B, Lichtman JW. 2004. Axon Branch Removal at Developing
584 Synapses by Axosome Shedding. *Neuron* **44**:651–661. doi:10.1016/j.neuron.2004.10.026

585 Bradley RM, Cao X, Akin T, Najafi K. 1997. Long term chronic recordings from peripheral sensory fibers
586 using a sieve electrode array. *J Neurosci Methods* **73**:177–186. doi:10.1016/S0165-
587 0270(97)02225-5
588 Breton-Provencher V, Bakhshetyan K, Hardy D, Bammann RR, Cavarretta F, Snapyan M, Côté D, Migliore
589 M, Saghatelyan A. 2016. Principal cell activity induces spine relocation of adult-born
590 interneurons in the olfactory bulb. *Nat Commun* **7**:12659. doi:10.1038/ncomms12659
591 Castillo D, Seidel K, Salcedo E, Ahn C, de Sauvage FJ, Klein OD, Barlow LA. 2014. Induction of ectopic
592 taste buds by SHH reveals the competency and plasticity of adult lingual epithelium.
593 *Development* **141**:2993–3002. doi:10.1242/dev.107631
594 Castillo-Azofeifa D, Losacco JT, Salcedo E, Golden EJ, Finger TE, Barlow LA. 2017. Sonic hedgehog from
595 both nerves and epithelium is a key trophic factor for taste bud maintenance. *Development*
596 **144**:3054–3065. doi:10.1242/dev.150342
597 Cuntz H, Forstner F, Borst A, Häusser M. 2010. One Rule to Grow Them All: A General Theory of
598 Neuronal Branching and Its Practical Application. *PLoS Comput Biol* **6**:e1000877.
599 doi:10.1371/journal.pcbi.1000877
600 De Paola V, Holtmaat A, Knott G, Song S, Wilbrecht L, Caroni P, Svoboda K. 2006. Cell Type-Specific
601 Structural Plasticity of Axonal Branches and Boutons in the Adult Neocortex. *Neuron* **49**:861–
602 875. doi:10.1016/j.neuron.2006.02.017
603 Donnelly CR, Kumari A, Li L, Vesela I, Bradley RM, Mistretta CM, Pierchala BA. 2022. Probing the
604 multimodal fungiform papilla: complex peripheral nerve endings of chorda tympani taste and
605 mechanosensitive fibers before and after Hedgehog pathway inhibition. *Cell Tissue Res* **387**:225–
606 247. doi:10.1007/s00441-021-03561-1
607 Donnelly CR, Shah AA, Mistretta CM, Bradley RM, Pierchala BA. 2018. Biphasic functions for the GDNF-
608 Ret signaling pathway in chemosensory neuron development and diversification. *Proc Natl Acad*
609 *Sci* **115**. doi:10.1073/pnas.1708838115
610 Dvoryanchikov G, Hernandez D, Roebber JK, Hill DL, Roper SD, Chaudhari N. 2017. Transcriptomes and
611 neurotransmitter profiles of classes of gustatory and somatosensory neurons in the geniculate
612 ganglion. *Nat Commun* **8**. doi:10.1038/s41467-017-01095-1
613 Ermilov AN, Kumari A, Li L, Joiner AM, Grachtchouk MA, Allen BL, Dlugosz AA, Mistretta CM. 2016.
614 Maintenance of Taste Organs Is Strictly Dependent on Epithelial Hedgehog/GLI Signaling. *PLOS*
615 *Genet* **12**:e1006442. doi:10.1371/journal.pgen.1006442
616 Erturk A, Hellal F, Enes J, Bradke F. 2007. Disorganized Microtubules Underlie the Formation of
617 Retraction Bulbs and the Failure of Axonal Regeneration. *J Neurosci* **27**:9169–9180.
618 doi:10.1523/JNEUROSCI.0612-07.2007
619 Farbman AI. 1980. RENEWAL OF TASTE BUD CELLS IN RAT CIRCUMVALLATE PAPILLAE. *Cell Prolif* **13**:349–
620 357. doi:10.1111/j.1365-2184.1980.tb00474.x
621 Gangadharan V, Zheng H, Taberner FJ, Landry J, Nees TA, Pistolic J, Agarwal N, Männich D, Benes V,
622 Helmstaedter M, Ommer B, Lechner SG, Kuner T, Kuner R. 2022. Neuropathic pain caused by
623 miswiring and abnormal end organ targeting. *Nature* **606**:137–145. doi:10.1038/s41586-022-
624 04777-z
625 Grutzendler J, Kasthuri N, Gan W-B. 2002. Long-term dendritic spine stability in the adult cortex. *Nature*
626 **420**:812–816. doi:10.1038/nature01276
627 Hamamichi R, Asano-Miyoshi M, Emori Y. 2006. Taste bud contains both short-lived and long-lived cell
628 populations. *Neuroscience* **141**:2129–2138. doi:10.1016/j.neuroscience.2006.05.061
629 Han J, Choi M. 2018. Comprehensive functional screening of taste sensation *in vivo* (preprint).
630 Neuroscience. doi:10.1101/371682
631 Hirose F, Takai S, Takahashi I, Shigemura N. 2020. Expression of protocadherin-20 in mouse taste buds.
632 *Sci Rep* **10**:2051. doi:10.1038/s41598-020-58991-8

633 Huang T, Ohman LC, Clements AV, Whiddon ZD, Krimm RF. 2021. Variable Branching Characteristics of
634 Peripheral Taste Neurons Indicates Differential Convergence. *J Neurosci* **41**:4850.
635 doi:10.1523/JNEUROSCI.1935-20.2021
636 Jacobsen AA, Aldahan AS, Hughes OB, Shah VV, Strasswimmer J. 2016. Hedgehog Pathway Inhibitor
637 Therapy for Locally Advanced and Metastatic Basal Cell Carcinoma: A Systematic Review and
638 Pooled Analysis of Interventional Studies. *JAMA Dermatol* **152**:816.
639 doi:10.1001/jamadermatol.2016.0780
640 Kinnamon JC, Sherman TA, Roper SD. 1988. Ultrastructure of mouse vallate taste buds: III. Patterns of
641 synaptic connectivity. *J Comp Neurol* **270**:1–10. doi:10.1002/cne.902700102
642 Kumari A, Ermilov AN, Allen BL, Bradley RM, Dlugosz AA, Mistretta CM. 2015. Hedgehog pathway
643 blockade with the cancer drug LDE225 disrupts taste organs and taste sensation. *J Neurophysiol*
644 **113**:1034–1040. doi:10.1152/jn.00822.2014
645 Kumari A, Ermilov AN, Grachtchouk M, Dlugosz AA, Allen BL, Bradley RM, Mistretta CM. 2017. Recovery
646 of taste organs and sensory function after severe loss from Hedgehog/Smoothened inhibition
647 with cancer drug sonidegib. *Proc Natl Acad Sci* **114**:E10369–E10378.
648 doi:10.1073/pnas.1712881114
649 Lacouture ME, Dréno B, Ascierto PA, Dummer R, Basset-Seguin N, Fife K, Ernst S, Licitra L, Neves RI, Peris
650 K, Puig S, Sokolof J, Sekulic A, Hauschild A, Kunstfeld R. 2016. Characterization and Management
651 of Hedgehog Pathway Inhibitor-Related Adverse Events in Patients With Advanced Basal Cell
652 Carcinoma. *The Oncologist* **21**:1218–1229. doi:10.1634/theoncologist.2016-0186
653 Lang S, Drouvelis P, Tafaj E, Bastian P, Sakmann B. 2011. Fast extraction of neuron morphologies from
654 large-scale SBFSEM image stacks. *J Comput Neurosci* **31**:533–545. doi:10.1007/s10827-011-
655 0316-1
656 Lee H, Macpherson LJ, Parada CA, Zuker CS, Ryba NJP. 2017. Rewiring the taste system. *Nature* **548**:330–
657 333. doi:10.1038/nature23299
658 Liebl DJ, Mbiene J-P, Parada LF. 1999. NT4/5 Mutant Mice Have Deficiency in Gustatory Papillae and
659 Taste Bud Formation. *Dev Biol* **213**:378–389. doi:10.1006/dbio.1999.9385
660 Lindemann B. 2001. Receptors and transduction in taste. *Nature* **413**:219–225. doi:10.1038/35093032
661 Lu W-J, Mann RK, Nguyen A, Bi T, Silverstein M, Tang JY, Chen X, Beachy PA. 2018. Neuronal delivery of
662 Hedgehog directs spatial patterning of taste organ regeneration. *Proc Natl Acad Sci* **115**:E200–
663 E209. doi:10.1073/pnas.1719109115
664 Lundy RF, Contreras RJ. 1999. Gustatory Neuron Types in Rat Geniculate Ganglion. *J Neurophysiol*
665 **82**:2970–2988. doi:10.1152/jn.1999.82.6.2970
666 Marshall KL, Clary RC, Baba Y, Orlowsky RL, Gerling GJ, Lumpkin EA. 2016. Touch Receptors Undergo
667 Rapid Remodeling in Healthy Skin. *Cell Rep* **17**:1719–1727. doi:10.1016/j.celrep.2016.10.034
668 Martineau É, Di Polo A, Vande Velde C, Robitaille R. 2018. Dynamic neuromuscular remodeling precedes
669 motor-unit loss in a mouse model of ALS. *eLife* **7**:e41973. doi:10.7554/eLife.41973
670 Meng L, Ohman-Gault L, Ma L, Krimm RF. 2015. Taste Bud-Derived BDNF Is Required to Maintain Normal
671 Amounts of Innervation to Adult Taste Buds. *eneuro* **2**:ENEURO.0097-15.2015.
672 doi:10.1523/ENEURO.0097-15.2015
673 Miller IJ, Reedy FE. 1990. Variations in human taste bud density and taste intensity perception. *Physiol*
674 *Behav* **47**:1213–1219. doi:10.1016/0031-9384(90)90374-D
675 Nakazawa S, Mizuno H, Iwasato T. 2018. Differential dynamics of cortical neuron dendritic trees
676 revealed by long-term in vivo imaging in neonates. *Nat Commun* **9**:3106. doi:10.1038/s41467-
677 018-05563-0
678 Nosrat IV, Margolskee RF, Nosrat CA. 2012. Targeted Taste Cell-specific Overexpression of Brain-derived
679 Neurotrophic Factor in Adult Taste Buds Elevates Phosphorylated TrkB Protein Levels in Taste

680 Cells, Increases Taste Bud Size, and Promotes Gustatory Innervation. *J Biol Chem* **287**:16791–
681 16800. doi:10.1074/jbc.M111.328476
682 Ohman LC, Hanbala L, Krimm RF. in submission. Taste arbor structural variability analyzed across taste
683 regions.
684 Ohman LC, Krimm RF. 2021. Variation in taste ganglion neuron morphology: insights into taste function
685 and plasticity. *Curr Opin Physiol* **20**:134–139. doi:10.1016/j.cophys.2020.12.011
686 Ohman-Gault L, Huang T, Krimm R. 2017. The transcription factor Phox2b distinguishes between oral
687 and non-oral sensory neurons in the geniculate ganglion. *J Comp Neurol* **525**:3935–3950.
688 doi:10.1002/cne.24312
689 Okubo T, Pevny LH, Hogan BLM. 2006. Sox2 is required for development of taste bud sensory cells.
690 *Genes Dev* **20**:2654–2659. doi:10.1101/gad.1457106
691 Patel AV, Krimm RF. 2010. BDNF is required for the survival of differentiated geniculate ganglion
692 neurons. *Dev Biol* **340**:419–429. doi:10.1016/j.ydbio.2010.01.024
693 Pfeiffer T, Poll S, Bancelin S, Angibaud J, Inavalli VK, Keppler K, Mittag M, Fuhrmann M, Nägerl UV. 2018.
694 Chronic 2P-STED imaging reveals high turnover of dendritic spines in the hippocampus in vivo.
695 *eLife* **7**:e34700. doi:10.7554/eLife.34700
696 PURVES D, HADLEY R. 1985. Changes in the dendritic branching of adult mammalian neurones revealed
697 by repeated imaging in situ. *Nat Lond* **315**:404–406.
698 Romanov RA, Lasher RS, High B, Savidge LE, Lawson A, Rogachevskaja OA, Zhao H, Rogachevsky VV,
699 Bystrova MF, Churbanov GD, Adameyko I, Harkany T, Yang R, Kidd GJ, Marambaud P, Kinnamon
700 JC, Kolesnikov SS, Finger TE. 2018. Chemical synapses without synaptic vesicles: Purinergic
701 neurotransmission through a CALHM1 channel-mitochondrial signaling complex. *Sci Signal*
702 **11**:eaao1815. doi:10.1126/scisignal.aao1815
703 Speidel CC. 1935. STUDIES OF LIVING NERVES: IV. GROWTH, REGENERATION, AND MYELINATION OF
704 PERIPHERAL NERVES IN SALAMANDERS. *Biol Bull* **68**:140–161. doi:10.2307/1537291
705 Speidel CC. 1933. Studies of living nerves. II. Activities of ameboid growth cones, sheath cells, and myelin
706 segments, as revealed by prolonged observation of individual nerve fibers in frog tadpoles. *Am J*
707 *Anat* **52**:1–79. doi:10.1002/aja.1000520102
708 Speidel CC. 1932. Studies of living nerves. I. The movements of individual sheath cells and nerve sprouts
709 correlated with the process of myelin-sheath formation in amphibian larvae. *J Exp Zool* **61**:279–
710 331. doi:10.1002/jez.1400610206
711 Sukumaran SK, Lewandowski BC, Qin Y, Kotha R, Bachmanov AA, Margolskee RF. 2017. Whole
712 transcriptome profiling of taste bud cells. *Sci Rep* **7**:7595. doi:10.1038/s41598-017-07746-z
713 Takahashi S, Ishida A, Kubo A, Kawasaki H, Ochiai S, Nakayama M, Koseki H, Amagai M, Okada T. 2019.
714 Homeostatic pruning and activity of epidermal nerves are dysregulated in barrier-impaired skin
715 during chronic itch development. *Sci Rep* **9**:8625. doi:10.1038/s41598-019-44866-0
716 Tang JY, Mackay-Wiggan JM, Aszterbaum M, Yauch RL, Lindgren J, Chang K, Coppola C, Chanana AM,
717 Marji J, Bickers DR, Epstein EH. 2012. Inhibiting the Hedgehog Pathway in Patients with the
718 Basal-Cell Nevus Syndrome. *N Engl J Med* **366**:2180–2188. doi:10.1056/NEJMoa1113538
719 Trachtenberg JT, Chen BE, Knott GW, Feng G, Sanes JR, Welker E, Svoboda K. 2002. Long-term in vivo
720 imaging of experience-dependent synaptic plasticity in adult cortex. *Nature* **420**:788–794.
721 doi:10.1038/nature01273
722 Treffy RW, Collins D, Hoshino N, Ton S, Katsevman GA, Oleksiak M, Runge EM, Cho D, Russo M, Spec A,
723 Gomulka J, Henkemeyer M, Rochlin MW. 2016. Ephrin-B/EphB Signaling Is Required for Normal
724 Innervation of Lingual Gustatory Papillae. *Dev Neurosci* **38**:124–138. doi:10.1159/000444748
725 Vandenbeuch A, Larson ED, Anderson CB, Smith SA, Ford AP, Finger TE, Kinnamon SC. 2015. Postsynaptic
726 P2X3-containing receptors in gustatory nerve fibres mediate responses to all taste qualities in

727 mice: Role of P2X3-containing receptors in taste. *J Physiol* **593**:1113–1125.
728 doi:10.1113/jphysiol.2014.281014
729 Verzé L, Paraninfo A, Ramieri G, Viglietti-Panzica C, Panzica GC. 1999. Immunocytochemical evidence of
730 plasticity in the nervous structures of the rat lower lip. *Cell Tissue Res* **297**:203–211.
731 doi:10.1007/s004410051348
732 Walsh MK, Lichtman JW. 2003. In Vivo Time-Lapse Imaging of Synaptic Takeover Associated with
733 Naturally Occurring Synapse Elimination. *Neuron* **37**:67–73. doi:10.1016/S0896-6273(02)01142-
734 X
735 Wilson CE, Lasher RS, Yang R, Dzowo Y, Kinnamon JC, Finger TE. 2022. Taste Bud Connectome:
736 Implications for Taste Information Processing. *J Neurosci* **42**:804. doi:10.1523/JNEUROSCI.0838-
737 21.2021
738 Wu A, Dvoryanchikov G, Pereira E, Chaudhari N, Roper SD. 2015. Breadth of tuning in taste afferent
739 neurons varies with stimulus strength. *Nat Commun* **6**:1–11.
740 Yarmolinsky DA, Zuker CS, Ryba NJP. 2009. Common Sense about Taste: From Mammals to Insects. *Cell*
741 **139**:234–244. doi:10.1016/j.cell.2009.10.001
742 Yee CL, Jones KR, Finger TE. 2003. Brain-derived neurotrophic factor is present in adult mouse taste cells
743 with synapses. *J Comp Neurol* **459**:15–24. doi:10.1002/cne.10589
744 Zaidi FN, Cicchini V, Kaufman D, Ko E, Ko A, Van Tassel H, Whitehead MC. 2016. Innervation of taste
745 buds revealed with Brainbow-labeling in mouse. *J Anat* **229**:778–790. doi:10.1111/joa.12527
746 Zaidi FN, Whitehead MC. 2006. Discrete Innervation of Murine Taste Buds by Peripheral Taste Neurons. *J*
747 *Neurosci* **26**:8243–8253. doi:10.1523/JNEUROSCI.5142-05.2006
748 Zeng H, Sanes JR. 2017. Neuronal cell-type classification: challenges, opportunities and the path
749 forward. *Nat Rev Neurosci* **18**:530–546. doi:10.1038/nrn.2017.85
750 Zhang J, Jin H, Zhang W, Ding C, O'Keeffe S, Ye M, Zuker CS. 2019. Sour Sensing from the Tongue to the
751 Brain. *Cell* **179**:392-402.e15. doi:10.1016/j.cell.2019.08.031
752

753